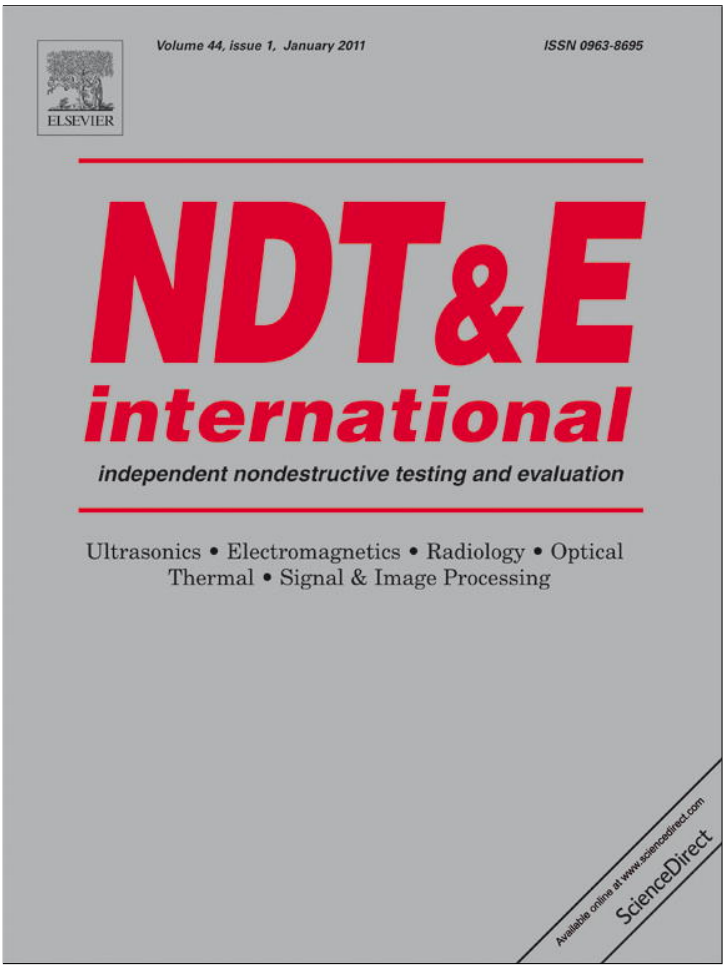

NDT&E International 44 (2011) 67–74

Contents lists available at ScienceDirect

NDT&E International

journal homepage: www.elsevier.com/locate/ndteint

Experimental study of nonlinear Rayleigh wave propagation in shot-peened aluminum plates—Feasibility of measuring residual stress

Minghe Liu [a], Jin-Yeon Kim [b], Laurence Jacobs [b,c,*], Jianmin Qu [a]

[a] Department of Civil and Environmental Engineering, Northwestern University, Evanston, IL 60208, USA
[b] School of Civil and Environmental Engineering, Georgia Institute of Technology, Atlanta, GA 30332-0355, USA
[c] GWW School of Mechanical Engineering, Georgia Institute of Technology, Atlanta, GA 30332-0405, USA

ARTICLE INFO

Article history:
Received 20 March 2010
Received in revised form
11 September 2010
Accepted 16 September 2010
Available online 22 September 2010

Keywords:
Residual stress
Nonlinear ultrasonics
Shot-peening

ABSTRACT

Shot-peening is widely used in the aerospace industry to enhance the resistance of structural components to fatigue damage and stress corrosion by putting the outside layer of a component under an initial, residual compressive stress. The ability to measure these near-surface residual stresses is useful from a quality control and certification perspective, and can help predict the fatigue life of shot-peened components. This paper presents experimental results to examine the feasibility of measuring near-surface residual stresses using nonlinear Rayleigh surface waves. Experiments are conducted on aluminum alloy (AA 7075) samples shot-peened at different peening intensities and thus with different levels of residual stresses. The surface roughness of these samples is also measured. The nonlinear ultrasonic results show a large increase in the acoustic nonlinearity parameter, indicating the potential of nonlinear ultrasonics for the in situ measurement of near-surface residual stresses. The effects of surface roughness and the driving frequency on the measured acoustic nonlinearity parameter are briefly discussed. Finally, a preliminary model is used to interpret some experimental results. Future work to evaluate the separate contributions of cold work, residual stress and surface roughness to the total measured nonlinearity is also discussed.

1. Introduction

Most ultrasonic techniques for evaluating residual stresses measure changes in ultrasonic wave velocities and then relate them to the state of the internal stresses (residual or applied) [1,2]. Since the maximum change in the ultrasonic wave velocity ($\Delta v/v_0$) is usually less than a few percentages, the accurate measurement of residual stress with this method requires a high-precision measurement system. Additional difficulties with these time-of-flight methods are that the ultrasonic velocity will also change due to the surface conditions such as the sub-surface texture and the roughness; changes in ultrasonic velocity due to these extraneous conditions are often of the same order as those due to the residual stresses [3]. As a result, the accurate measurement of residual stresses with an ultrasonic velocity measurement is often a difficult task.

New physical models [4–6] provide the theoretical background for using nonlinear ultrasonics to measure plastic deformation in metals. The microplastic deformation that appears in the form of dislocation substructures does not cause a large change in the macroscopic properties such as elastic moduli, ultrasonic velocities or attenuation. However, these new models predict that the accumulation of dislocations and the associated residual stresses cause appreciable nonlinear distortions of ultrasonic waves, thereby generating higher harmonic components in an initially monochromatic ultrasonic signal. For this reason, nonlinear ultrasonic waves can be used to quantify the dislocation density (microplasticity) in metals, and thus be used to measure fatigue damage in a quantitative fashion.

Recently, reliable experimental techniques for nonlinear ultrasonic measurements have been developed and applied to characterize fatigue damage in various metals including nickel-base superalloys and aluminum [7–14]. In all these experiments, what is really being measured by the nonlinear ultrasound is the microplasticity or the plastic deformation, as is shown in [7–10] and theoretically demonstrated in [4–6]. On this basis, the current research applies these nonlinear ultrasonic techniques to measure near-surface plasticity and the residual stresses associated with shot-peening. Note that both the near-surface plastic deformation and residual stresses independently affect the nonlinear properties of the surface layer. Shot-peening is widely used in the aerospace industry to enhance the resistance of structural components to fatigue damage and stress corrosion by putting the outside layer of a component under an initial, residual compressive stress. Note that shot-peening causes three different

* Corresponding author at: School of Civil and Environmental Engineering, Georgia Institute of Technology, Atlanta, GA 30332-0355, USA.
E-mail address: laurence.jacobs@ce.gatech.edu (L. Jacobs).

0963-8695/$ - see front matter © 2010 Elsevier Ltd. All rights reserved.
doi:10.1016/j.ndteint.2010.09.008

effects: residual stress, cold work and surface roughness. Cold work includes surface texture and the associated increase in dislocation density.

The objective of this research is to determine the sensitivity of nonlinear Rayleigh surface waves to changes in the surface conditions made by shot-peening, as a first step toward a quantitative measurement of the residual stresses in shot-peened samples. Rayleigh surface waves are ideally suited for this purpose since their ultrasonic energy is confined to the near-surface layer where the residual stresses are most concentrated. Ultrasonic measurements are made on aluminum samples that are shot-peened at different peening intensities. These preliminary experimental results demonstrate the high sensitivity of the measured ultrasonic nonlinearity parameter to variations in surface condition. The effect of surface roughness – a critical factor in the ultrasonic velocity measurement – is also investigated and the numerical results from a simplified model are used to evaluate and interpret the experimental data. Experiments at different fundamental frequencies are also conducted to examine the effect of frequency on the measured acoustic nonlinearity.

2. Rayleigh surface waves and nonlinear acoustic parameter

The equations of motion of a solid in the absence of body forces are written in material coordinates, $\boldsymbol{X}$, as

$$\rho\frac{\partial^2 u_i}{\partial t^2}=\frac{\partial \sigma_{ij}}{\partial X_j}, \tag{1}$$

where ρ is the mass density, u_i the displacement vector, t time and σ_{ij} the stress tensor. The plasticity and residual stresses lead to a relation between the first Piola–Kirchhoff stresses, σ_{ij} and the displacement gradients as

$$\sigma_{ij}=\sigma^0_{ij}+A_{ijkl}\frac{\partial u_k}{\partial X_l}+\frac{1}{2}A_{ijklmn}\frac{\partial u_k}{\partial X_l}\frac{\partial u_m}{\partial X_n}+\cdots \tag{2}$$

where σ^0_{ij} are the residual stresses in the material, A_{ijkl} and A_{ijklmn} are the second- and third-order Huang coefficients [4] and are related to the corresponding second- and third-order elastic constants in the standard notation by $A_{ijkl}=\sigma^0_{jl}\delta_{ik}+\overline{C}_{ijkl}$ and $A_{ijklmn}=\overline{C}_{ijklmn}+\overline{C}_{jlmn}\delta_{ik}+\overline{C}_{ijnl}\delta_{km}+\overline{C}_{jnkl}\delta_{im}$. $\overline{C}_{ijkl}$ and $\overline{C}_{ijklmn}$ are modified by fatigue damage (dislocation substructures [4]) from their initial values, C_{ijkl} and C_{ijklmn}. Expressions for the modified elastic constants during fatigue have been presented in terms of the residual stress and plastic strain [6]. The density of a material undergoing finite deformation is given by $\rho=\rho_0/\det\mathbf{F}$ where ρ_0 is the constant density in the unstressed configuration, and $\boldsymbol{F}$ the deformation gradient tensor, defined as $F_{ij}=\delta_{ij}+\partial u_j/\partial X_i$. Substituting Eq. (2) into Eq. (1) and considering one-dimensional wave propagation of a longitudinal wave in an isotropic solid yields

$$\frac{\partial^2 u_1}{\partial t^2}=c^2\frac{\partial^2 u_1}{\partial X_1^2}\left[1-\beta\frac{\partial u_1}{\partial X_1}\right] \tag{3}$$

where $c=\sqrt{(\overline{C}_{1111}+\sigma^0_{11})/\rho}$ is the longitudinal wave speed and β the acoustic nonlinearity parameter defined as

$$\beta=-\frac{\overline{C}_{111111}+3\overline{C}_{1111}}{\overline{C}_{1111}+\sigma^0_{11}}. \tag{4}$$

In Eq. (4), the residual stress σ^0_{11} increases with the increment in shot-peening intensity, but it is relatively small compared to the elastic constants. The effective second-order elastic constant $\overline{C}_{1111}$ has a negligible dependence on plastic deformation while the third-order elastic constant $\overline{C}_{111111}$ depends strongly on the plastic deformation (or the dislocation density) that has occurred in the medium. Although the actual relationship is rather complicated, β generally increases with increasing plastic deformation.

During shot-peening, the material's surface layer undergoes plastic deformation. The amount and the extent of plastic deformation increase with an increase in peening intensity. It is thus conceivable that the shot-peening induced surface plasticity, which is proportional to the compressive surface residual stress, can be evaluated from the measured nonlinear acoustic parameter β. This paper uses Rayleigh waves to measure β, thus characterizing the surface residual stresses.

Consider a Rayleigh wave near the free surface of a half-space. It has been shown [8] that

$$\beta=\frac{8u_{2\omega}}{\omega^2X_1u_\omega^2}\frac{c_L\cdot\sqrt{c_L^2-c_R^2}}{2(c_T/c_R)^2-1} \tag{5}$$

where X_1 is the distance of Rayleigh wave propagation, u_ω and $u_{2\omega}$ are the out-of-plane displacement amplitudes of the fundamental and second-order harmonics, respectively, c_L, c_T and c_R are, respectively, the longitudinal, shear and Rayleigh wave speeds in the solid, and ω is the angular frequency. The experiments in this research measure this relative acoustic nonlinearity parameter, $u_{2\omega}/u_\omega^2$ (or normalized second harmonic), as a function of increasing propagation distance (X_1), and then the slope with respect to X_1 is taken as the relative parameter that is proportional to the absolute acoustic nonlinearity parameter, β, for a fixed frequency. This investigation also uses the ratio, $u_{2\omega}/u_\omega^2f^2$, where f is the driving fundamental frequency, to compare the absolute nonlinearity parameters at different frequencies. The slope of this ratio over propagation distance (X_1), should also be proportional to the absolute acoustic nonlinearity parameter, i.e., $u_{2\omega}/u_\omega^2f^2\sim\beta$ (see Eq. (5)).

3. Sample preparation and experimental setup

3.1. Sample Preparation

Three aluminum alloy AA 7075 samples (304.8 mm × 101.6 mm and 25.4 mm thick) with different levels of residual stress are prepared. One sample is kept as a reference (as-received) sample. The other two samples are commercially shot-peened at the Almen intensities of 8 A and 16 A, both with 0.023 in. (0.584 mm) diameter cast steel balls and 100% coverage. The reference sample is lightly polished with a fine sand paper and lubrication oil to remove any accumulated dirt and machine scratches from the surface.

Fig. 1 shows the typical depths and profiles of residual stresses measured using X-ray diffraction for AA 7075 surfaces shot-peened at Almen intensities of 8 A and 16 A with cast steel balls with diameters of 0.023–0.028 in. (0.584–0.711 mm) and 100% coverage [15]. This figure shows that the maximum penetration depth is about 600 μm for the 16 A sample. The first set of ultrasonic experiments in the current research uses a wavelength of 1.3 mm (the Rayleigh wave speed is 2920 m/s in AA 7075 and the driving frequency is 2.25 MHz); thus the Rayleigh surface wave energy covers the entire depth of the residual stresses.

3.2. Experimental setup

A schematic of the nonlinear ultrasonic measurement setup is shown in Fig. 2. A high power gated amplifier RAM-5000 Mark IV (RITEC Inc, Warwick, RI) is used for the generation of nonlinear Rayleigh surface waves. As shown in [7,8], the input voltage level

needs to be sufficiently high in order to make a reliable nonlinear ultrasonic measurement; this study uses a voltage at 90% of the maximum output level of the amplifier (~734 Vpp with the transducer loading). A 25 cycle tone burst signal is used to obtain a sufficient length of steady-state portion in the measured time-domain signal.

Commercial narrow-band piezoelectric transducers having center frequencies of 2.25 and 5 MHz are used as the transmitter and the receiver, respectively. Wedges are specially designed and manufactured from a Plexiglas block to launch and detect Rayleigh waves in the aluminum samples. The transducers are coupled to the wedges with light lubrication oil and these transducer/wedge assemblies are coupled to the sample using the same couplant. Measurements are performed at multiple propagation distances, X_1, that vary from 30 to 200 mm.

This experimental setup provides a detection system that measures a voltage signal proportional to the out-of-plane (normal) surface displacement. The received signals are low-pass filtered with a cut-off frequency of 20.4 MHz and then sent to an oscilloscope (Tektronix TDS 420) that records these signals with a sampling frequency of 25 MHz and 15,000 sample points. 512 signals are averaged to increase the signal-to-noise ratio (SNR). The digitized time-domain signal is then transferred to a PC through the GPIB for post-signal processing. The internal trigger signal from the RAM-5000 amplifier is used as a reference trigger.

Fig. 3(a) shows a typical Rayleigh wave signal, generated and detected with the wedge transducers at a propagation distance of 180 mm. The entire length of this time-domain signal consists of a transient part (2 cycles) at the beginning, a steady-state portion (21 cycles), and the transient turn-off ringing at the end. A Hann window is imposed on the steady-state part of the signal, and a fast Fourier transform (FFT) is performed on the windowed signal. Fig. 3(b) shows the amplitudes of the fundamental (A_1) and second harmonic (A_2) in the frequency domain. Note that these uncalibrated electrical signal amplitudes A_1 and A_2 are proportional to the surface normal displacements, u_ω and $u_{2\omega}$ so that $u_{2\omega}/u_\omega^2 f^2 \sim A_2/A_1^2 f^2 \sim \beta$. In Fig. 3(b), the second harmonic amplitude is well above the noise level, even though its magnitude is about 20 times lower than that of the fundamental amplitude.

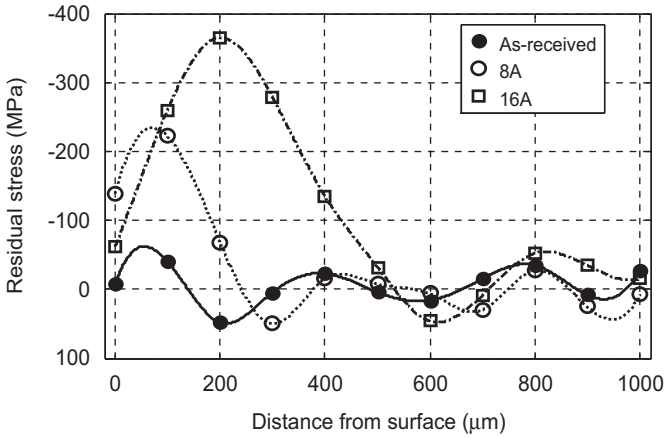

Fig. 1. Distribution of residual stresses in as-received and shot-peened samples [15].

4. Results and discussion

4.1. Acoustic nonlinearity of shot-peened samples

The measured relative acoustic nonlinearity parameters, A_2/A_1^2 (or normalized second harmonic amplitudes), versus the propagation distance for these three samples are shown in Fig. 4. Eq. (5) shows that the slope of A_2/A_1^2 versus the propagation distance is proportional to β. Error bars in this and the following figures represent the maximum range of variation in the measured slopes, and are obtained from three independent measurements. Note that the major source of these errors is the coupling variability. The maximum coupling variability calculated from the error bars is 5.6% for the as-received sample surface. For the shot-peened surface, the error bars are larger (11.5% for 16 A) due to the increased surface roughness. Fig. 4 clearly shows that the slope increases for samples with higher shot-peen intensity; the slopes for the 8 and 16 A samples are about 81% and 115% larger, respectively, than the as-received, reference sample. This large change in the measured acoustic nonlinearity parameter is due to

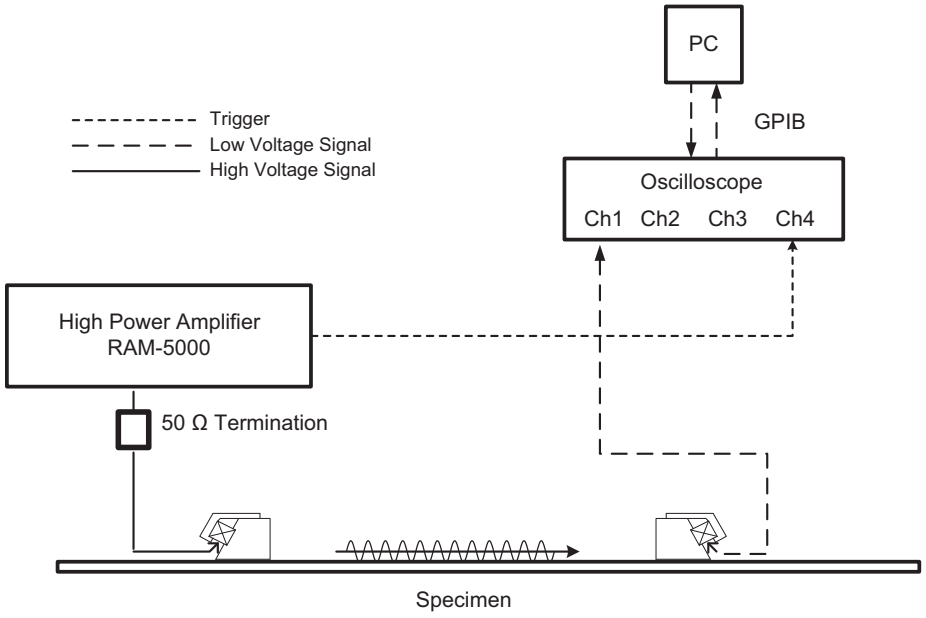

Fig. 2. Experimental setup.

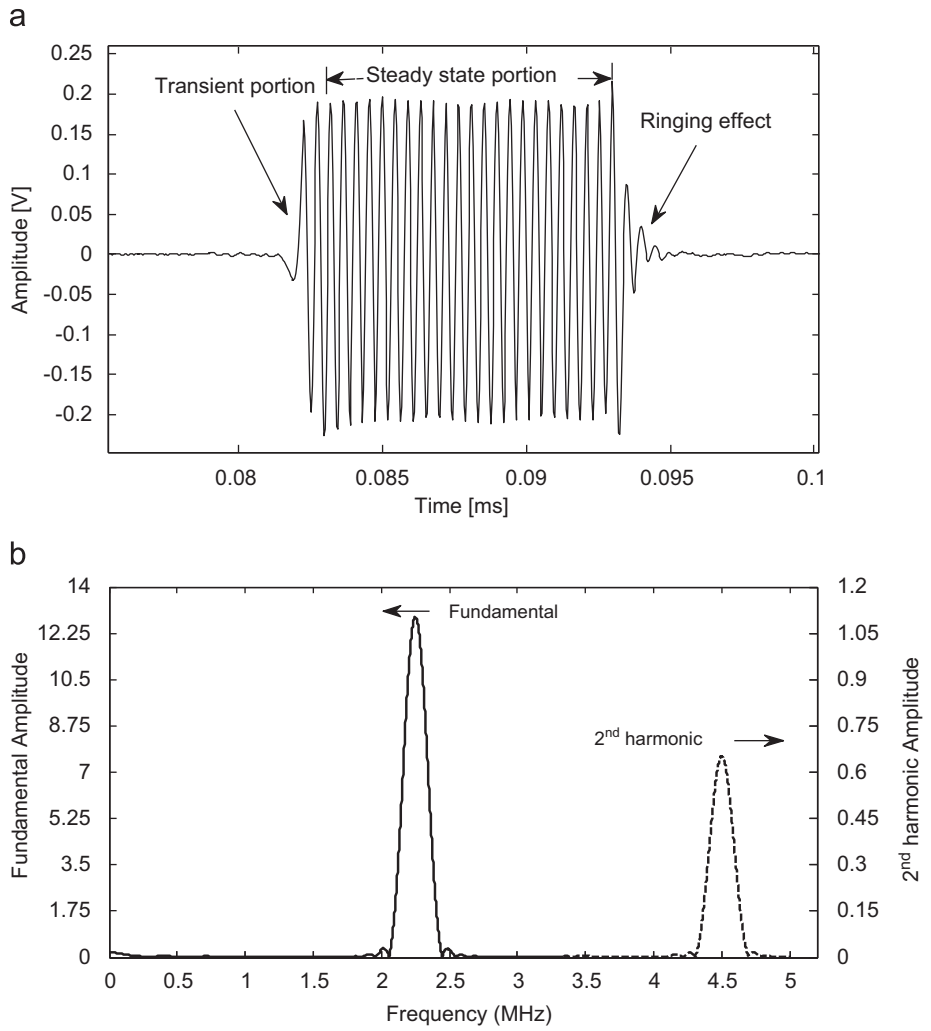

Fig. 3. (a) Time-domain signal; (b) Fourier spectrum (FFT) that shows the amplitudes of the fundamental and second harmonic (at a propagation distance of 180 mm).

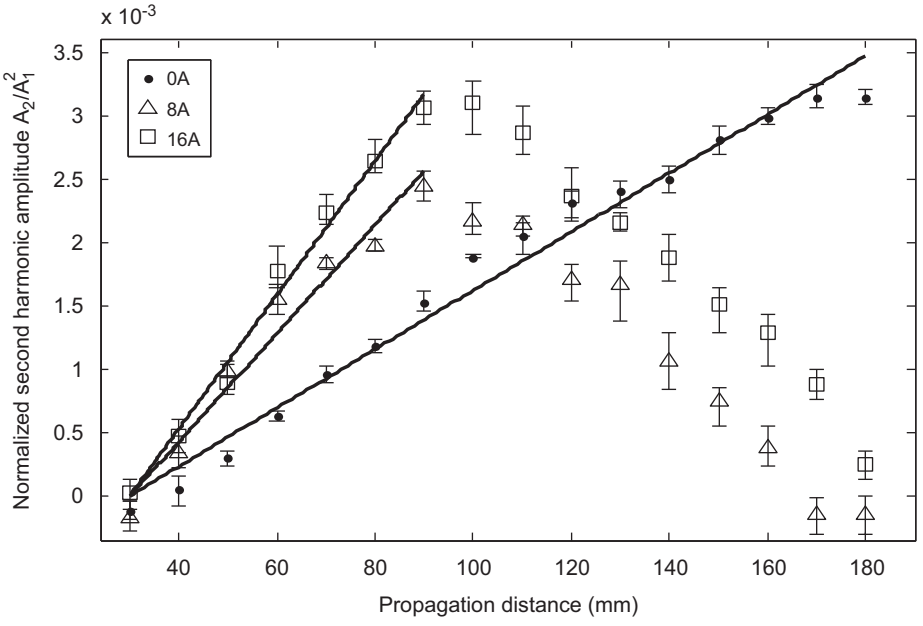

Fig. 4. Variation in the normalized second harmonic amplitude as a function of propagation distance for the reference sample (0 A), samples shot-peened at intensities 8 and 16 A. The frequency of excitation is 2.25 MHz.

the combined effect of residual stress from the shot-peening (and its associated plastic deformation), cold work and any additional surface roughness. It is worth mentioning that the cold work effect in shot-peening does not cause significant velocity changes from previous measurements [3]. Another set of experiments, discussed in the next section, are performed to determine the effects of the surface roughness on the measured acoustic nonlinearity. Another effect of surface roughness is the attenuation of surface waves. This attenuation causes a decrease or downturn of the nonlinearity parameter with increase in propagation distance in the relative acoustic nonlinearity parameter (A_2/A_1^2) at propagation distances of about 90 and 100 mm as shown in Fig. 4.

The changes in ultrasonic wave velocity are also measured as part of the nonlinear measurements. The Rayleigh surface wave velocity changes from 2921 to 2892 and 2855 m/s for the 8 and 16 A samples, respectively, and these correspond to a decrease by 1.0% and 2.3%. These measured velocities are at the fundamental frequency (2.25 MHz). Lavrentyev and Veronesi [3] showed that about 50% of the velocity change is typically due to the surface roughness. Therefore, one can estimate the actual change in the surface wave velocity due to the residual stress to be less than 1%, since the 1% decrease is caused by all the other effects such as residual stress, texture and plastic deformation. These results show that the relative acoustic nonlinearity parameter is much more sensitive than the ultrasonic velocity to the changes in surface condition due to shot-peening.

Table 1
Average surface roughness (Ra), root mean square roughness (Rq) and peak to valley ratio (PV) of AA 7075 samples shot-peened at different Almen intensities.

Peening intensity (A)	Average surface roughness (Ra, μm)	Root mean square roughness (Rq, μm)	Peak to valley ratio
0	1.73	2.13	116.19
8	4.906	6.205	144.396
8 polished	3.549	4.473	39.30
16	7.501	9.511	146.602

4.2. Effects of the removal of the thin outer layer

It is known that the rough surface of a shot-peened component can significantly (negatively) influence ultrasonic velocity measurements. In the meantime, the penetration depth of the major cold work where the dislocation density is excessively high is confined in a thin layer whose thinness is about one-third the depth of residual stress. A non-contact optical profilometer (NewView 6200 3D Optical Profiling System manufactured by the Zygo Corporation) is used to measure surface roughness. The corresponding roughness parameters for the three samples are shown in Table 1.

The sample shot-peened at 8 A is hand-polished using fine polish papers (grit # 600, 800, 1200), and the nonlinear Rayleigh wave measurements are repeated on this sample. Fig. 5 compares the results of this sample before and after polishing, as well as for the as-received, reference sample. The slope for the polished shot-peened 8 A sample (called 8 AP) is reduced from 81% before polishing to 44.5% above that of the reference sample. Note that the polishing most likely removes some regions of high microplasticity. However, an increase of 44.5% is still significant, especially when compared to those changes obtained by the ultrasonic velocity method. The fluctuation in the measured nonlinear data is most likely due to some non-uniformity of the surface roughness caused by the hand polishing. This non-uniformity is easily confirmed from the non-uniform reflectivity of light from the surface. It is difficult to make a conclusion from this result since none of the contributing effects are completely removed. Nonetheless, a significant part of the surface roughness and some part of the near surface layer of excess cold work with high dislocation density, and thus high nonlinearity, are removed, which is believed to lead to this significant reduction in acoustic nonlinearity (from 81% to 44.5%) observed in this measurement. This qualitative statement is of course subject to a further experimental validation.

On the other hand, the smoother surface and its associated reduction in attenuation extends the range of the linear relationship between the relative acoustic nonlinearity and the propagation distance in the 8 AP sample; Fig. 5 shows a longer linear relationship for the 8 AP sample than the 8 A sample, where the

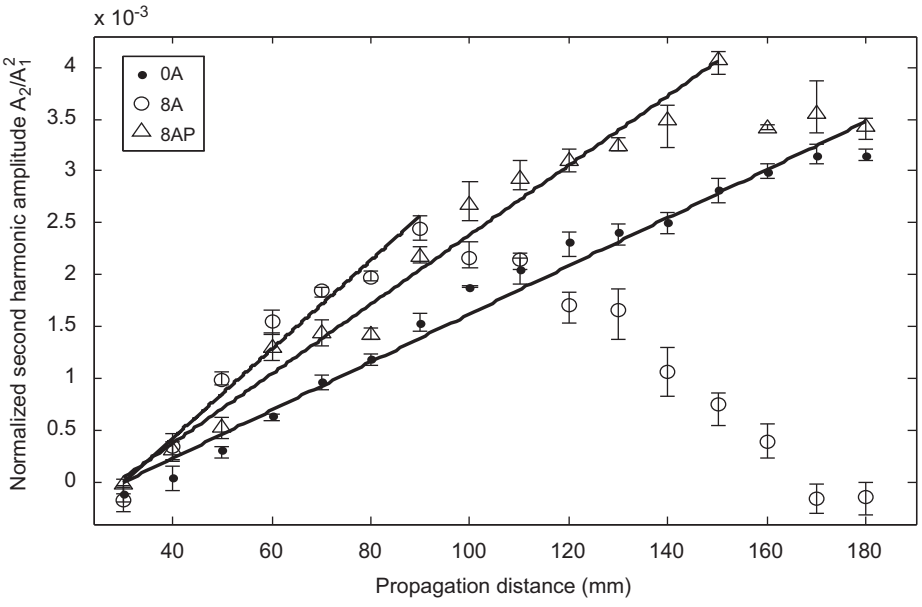

Fig. 5. Variation in the normalized second harmonic amplitude as a function of propagation distance for the reference sample (0 A), 8 A sample and polished 8 A sample (8 AP). The excitation frequency is 2.25 MHz.

propagation distance at which the "downturn" in this relationship occurs moves from 90 to 150 mm.

4.3. Effects of frequency on the measured acoustic nonlinearity

The frequency is an important factor in these acoustic nonlinearity measurements because of both the penetration depth and surface roughness-induced attenuation. Since the measured nonlinear parameter, β, represents an average of the material nonlinearity of about one wavelength beneath the surface, the results presented thus far contain the coupled effects of both the third-order elastic constant within the bulk material and the shot-peening induced plastic deformation and residual stress, which is limited to a thin layer near the surface as shown in Fig. 1. Since higher frequency Rayleigh waves tend to focus more energy near the surface, it is thus feasible to use Rayleigh waves at different frequencies to obtain β averaged over different regions near the surface. Additional measurements are performed on the reference sample (0 A), polished 8 A (8 AP) and 16 A samples at the driving frequencies of 1.5 and 2 MHz to explore the potential of using different driving frequencies to measure the depth dependance of β.

It is known that surface roughness causes dispersion of an otherwise nondispersive Rayleigh surface wave. However, the velocity change is less than 0.2% for the frequency changes considered here; thus the wedge angle is kept constant for all the measurements.

Fig. 6 shows the slopes of the ratio, $A_2/(A_1^2 f^2)$, as a function of propagation distance. This ratio, according to Eq. (5), should be independent of frequency if the measured β is the same. For the driving frequency of 1.5 MHz, the slopes of the ratio for the 8 AP and the 16 A samples are about 8% and 21%, respectively, larger than that of the as-received reference sample, while for the driving frequency of 2 MHz, they are about 23% and 52%, respectively, larger than that of the as-received sample.

Comparisons of the different slopes are plotted in Fig. 7. It is clearly seen that the slope, which represents the measured β, increases with increase in frequency on the same sample. As discussed earlier, the measured β is an average over the surface layer where the Rayleigh wave penetrates. Since higher frequency waves have smaller wavelengths, they penetrate less. For all three frequenies used here, their penetration depths are all larger than the depth where the maximum residual stress occurs. Therefore, less penetration depth would mean higher average β. This is consistent with the measurement results shown in Fig. 7, where higher frequencies result in higher measured average β.

Following the discussions above, by gradually increasing the frequency, one can obtain the residual stress distribution in the depth direction. Unfortunately, high-frequency waves also attenuate faster, which means shorter propagation distances for the second-order harmonic, which leads to reduced SNR. This is seen in Fig. 6, where the amplitude of the second-order harmonic loses its proportionality with propagation distance at much shorter propagation distances at 2 MHz than at 1.5 MHz. Note that for

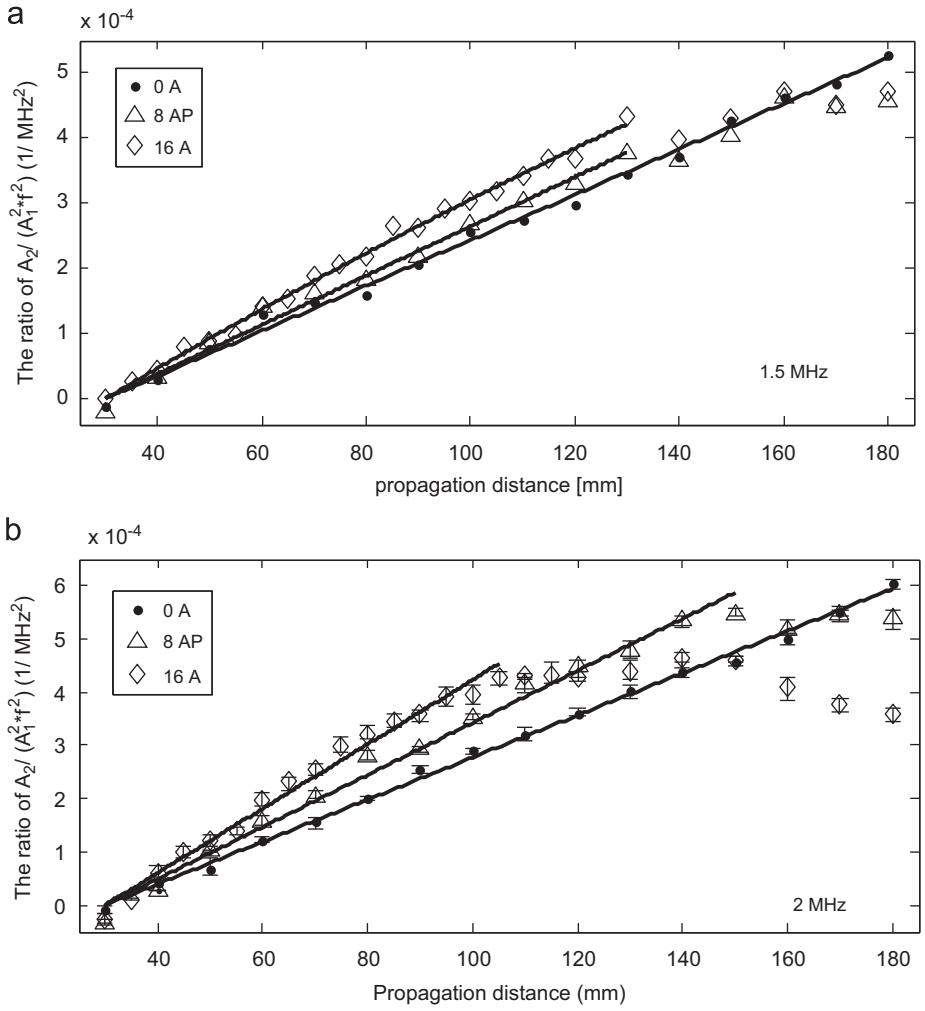

Fig. 6. The ratio, $A_2/(A_1^2 f^2)$, as a function of propagation distance for the reference sample (0 A), 8 AP sample and 16 A sample; (a) 1.5 and (b) 2 MHz.

frequencies higher than 2.25 MHz, the larger attenuation causes an unacceptable SNR, leading to inconsistencies in the measured acoustic nonlinearity.

4.4. Effect of attenuation

To account for attenuation, consider a quasilinear theory for Rayleigh-wave harmonic generation that calculates the out-of-plane displacements excited by an arbitrary two-dimensional source, taking the diffraction and attenuation effects into account

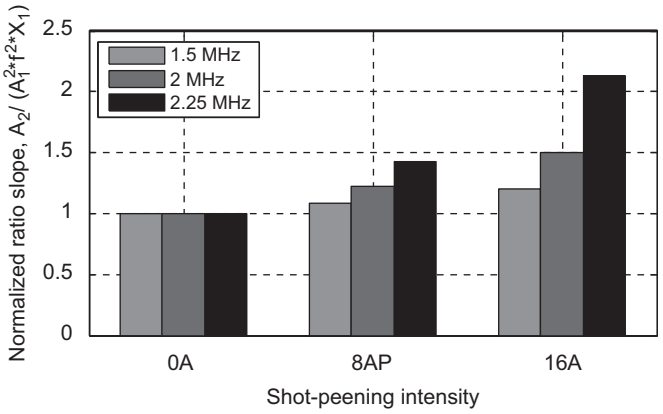

Fig. 7. The ratio slope, $A_2/(A_1^2 f^2 X_1)$ (see Eq. (5)), normalized by their reference (0 A) value at various frequencies for the reference sample (0 A), polished shot-peened with the intensity of 8 A (8 AP) and shot-peened with intensity of 16 A.

[16]. From this simulation, one can compare surface conditions from the estimated attenuation coefficients and predict the second harmonic generation. In this preliminary simulation, it is assumed that the properties including the acoustic nonlinearity and attenuation of the substrate medium are uniform. Consider a Rayleigh wave beam in an isotropic solid that occupies the half-space $z \le 0$ and propagates towards the $+x$ direction with its particle motion in the y direction. When diffraction is taken into account within the parabolic approximation, the spectral equation describing the propagation of nonlinear Rayleigh wave beams is derived. Only the relevant equations are summarized briefly here; for a full discussion see Ref. 16. Based on the spectral equation mentioned earlier, for the quasilinear system, the fundamental and second-harmonic components can be obtained by solving two equations [16] as follows:

$$\left(\frac{\partial}{\partial x} + \frac{1}{2ik_0}\frac{\partial^2}{\partial y^2} + \alpha_1\right) v_1 = 0, \tag{6}$$

$$\left(\frac{\partial}{\partial x} + \frac{1}{4ik_0}\frac{\partial^2}{\partial y^2} + \alpha_2\right) v_2 = -\frac{B_{11}k_0}{2c_R} v_1^2, \tag{7}$$

where c_R is the sound speed, $k_0=(\omega_0/c_R)$ the wave number, v_n the particle velocity (v_1 and v_2 are the first and second harmonic particle velocities) and $B_{11}=4\mu R_{11}/\zeta\rho c_R^2$ the coefficient of nonlinearity, in which μ is the shear modulus and R_{11} and ζ are defined elsewhere [16]. Select $B_{11}=0.22$ [17] in these numerical calculations. α_n is the attenuation coefficient at frequency $n\omega_0$.

The curves in Fig. 8 show the measured and calculated fundamental and second harmonic amplitudes for the 8 A and

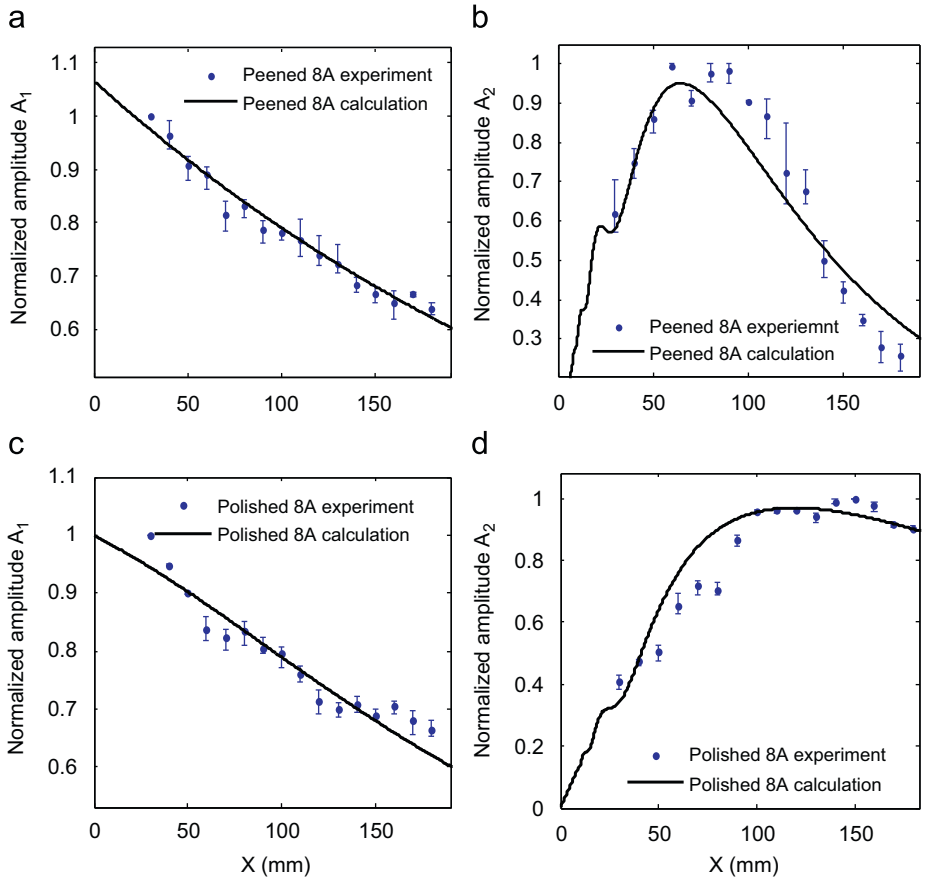

Fig. 8. Normalized surface normal displacements along the beam axis: (a) fundamental and (b) second harmonic amplitudes in the 8 A sample with $\alpha_1=2.0$ at the fundamental frequency and $\alpha_2=22.5$ at the second harmonic frequency; (c) fundamental and (d) second harmonic amplitudes in the 8 AP sample with $\alpha_1=1.63$ at the fundamental frequency and $\alpha_2=5$ at the second harmonic frequency.

8 AP samples. This calculation is based on the finite difference method. One conclusion from this figure is that the downturn in the measured nonlinearity parameter is due to the roughness-induced attenuation. It is seen that the propagation distance, X_1 where the downturn appears is a larger distance when the surface is smoother (8 AP). Note that all the amplitudes including experimental points indicated by dots (with error bars) and the numerical calculations designated by the solid lines are normalized by their corresponding maximum values. Changes in α_1 and α_2 modify the curve's shape, and a least-squares fit of the fundamental and second harmonic amplitudes yields the most likely values of α_n. Due to the beam divergence, the fundamental amplitude decreases with the propagation distance, while the second harmonic increases up to a certain point and then starts decreasing. Note that the second harmonic attenuation coefficients α_2 in the 8 AP sample (5) is much smaller than in the 8 A sample (22.5) as a result of the polish.

5. Conclusion and future work

This preliminary research investigates the feasibility of using nonlinear Rayleigh surface waves to determine the near-surface residual stresses in shot-peened samples. The second harmonic amplitudes of Rayleigh surface waves are measured in AA 7075 samples shot-peened at different Almen intensities. The nonlinear ultrasonic results show a large increase in the acoustic nonlinearity parameter with an increase in intensity of shot-peening, indicating the potential of nonlinear ultrasonics for the in situ characterization of near-surface residual stresses. The inherent surface roughness of a specimen has a negative impact on this nonlinear ultrasonic measurement; this is also the case for linear surface wave velocity measurements. Measured changes in the relative acoustic nonlinearity are still significant, even after removing the surface roughness. However, this increase can be due to three different effects: residual stress, microplasticity (dislocations), and texture. It is thought that while the texture effect can be of minor importance, the microplasticity will have a large influence. In order to evaluate the residual stress, a systematic procedure needs to be developed to separate these different effects.

Future work should focus on separating the effects of cold work, residual stress and surface roughness. One possible way to do this is with annealing. The residual stress and cold work effects will be gradually removed by the gradual heat treatment in a protective atmosphere. Typically, the penetration depth of the excess cold work is only one-third of the penetration depth of the residual stress [18]. As a shallow sub-surface region exhibits a higher rate of relaxation and recrystallization than deeper regions, close to the surface, recrystallization starts at lower temperatures and occurs faster than at larger depths. Therefore, during annealing from a low to high temperature, cold work and part of the residual stress will be removed first, and then significant residual stress will be gradually removed at higher temperatures. After annealing, the only effect left is the surface roughness. By measuring the nonlinearity parameter continuously during this annealing process, one can evaluate separate contributions from these three different effects.

Acknowledgement

This work was partially supported by funds from the Georgia Tech-Boeing Strategic Alliance on Aerospace Manufacturing for the 21st Century, by National Science Foundation under CMMI-0653883 and by Air Force Office of Scientific Research under contract number FA9550-08-1-0241.

References

[1] Thompson RB, Lu WY, Clark AV. Handbook of measurement of residual stress. Fairmont Press; 1996.
[2] Thurston RN. Effective elastic coefficients for wave propagation in crystals under stress. J Acoust Soc Am 1965;37(2):348–56.
[3] Lavrentyev AI, Veronesi WA. Ultrasonic measurement of residual stress in shot peened aluminum alloy. In: Thompson DO, Chimenti DE, editors. Review of progress in quantitative non destructive evaluation, vol. 20. American Institute of Physics, 2001. p. 1472–79.
[4] Cantrell JH. Substructural organization, dislocation plasticity and harmonic generation in cyclically stressed wavy slip metals. Proc R Soc London A Math 2004;460(2043):757–80.
[5] Cantrell JH. Quantitative assessment of fatigue damage accumulation in wavy slip metals from acoustic harmonic generation. Philos Mag 2006;86(11):1539–54.
[6] Kim JY, Qu J, Jacobs LJ, Littles JW, Savage MF. Acoustic nonlinearity parameter due to microplasticity. J Nondestr Eval 2006;25(1):29–37.
[7] Kim JY, Jacobs LJ, Qu JM, Littles JW. Experimental characterization of fatigue damage in a nickel-base superalloy using nonlinear ultrasonic waves. J Acoust Soc Am 2006;120(3):1266–73.
[8] Herrmann J, Kim JY, Jacobs LJ, Qu JM, Littles JW, Savage MF. Assessment of material damage in a nickel-base superalloy using nonlinear Rayleigh surface waves. J Appl Phys 2006;99(12):124913.
[9] Pruell C, Kim JY, Qu J, Jacobs LJ. Evaluation of plasticity driven material damage using Lamb waves. Appl Phys Lett 2007;91:231911.
[10] Pruell C, Kim JY, Qu JM, Jacobs LJ. Evaluation of fatigue damage using nonlinear guided waves. Smart Mater Struct 2009;18:035003.
[11] Bermes C, Kim JY, Qu JM, Jacobs LJ. Experimental characterization of material nonlinearity using lamb waves. Appl Phys Lett 2007;90(2):021901.
[12] Bermes C, Kim JY, Qu JM, Jacobs LJ. Nonlinear Lamb waves for the detection of material nonlinearity. Mech Syst Signal Process 2008;22(3):638–46.
[13] Pruell C, Kim JY, Qu J, Jacobs LJ. A nonlinear-guided wave technique for evaluating plasticity-driven material damage in a metal plate. NDT E Int 2009;42(3):199–203.
[14] Shui G, Kim JY, Qu J, Wang YS, Jacobs LJ. A new technique for measuring the acoustic nonlinearity of materials using rayleigh waves. NDT E Int 2008;41(5):326–9.
[15] Honda T, Ramulu M, Kobayashi AS. Fatigue of shot peened 7075-T7351 SENB specimen—a 3-D analysis. Fatigue Fract Eng M 2006;29(6):416–24.
[16] Shull DJ, Kim EE, Hamilton MF, Zabolotskaya EA. Diffraction effects in nonlinear rayleigh-wave beams. J Acoust Soc Am 1995;97(4):2126–37.
[17] Hurley DC. Nonlinear propagation of narrow-band Rayleigh waves excited by a comb transducer. J Acoust Soc Am 1999;106(4):1782–8.
[18] Ruiz A, Nagy PB. SAW dispersion measurements for ultrasonic characterization of surface-treated metals. Instrum Meas Metrol 2003;3:59–85.